Nanomolar concentration of NSC606985, a camptothecin analog, induces leukemic-cell apoptosis through protein kinase Cδ–dependent mechanisms

Man-Gen Song, Shen-Meng Gao, Ke-Ming Du, Min Xu, Yun Yu, Yu-Hong Zhou, Qiong Wang, Zhu Chen, Yuan-Shan Zhu, and Guo-Qiang Chen

As a promising new class of anticancer drugs, camptothecins have advanced to the forefront of several areas of therapeutic and developmental chemotherapy. In the present study, we report that NSC606985, a rarely studied camptothecin analog, induces apoptosis in acute myeloid leukemia (AML) cells NB4 and U937 and inhibits the proliferation without cell death in breakpoint cluster region–Abelson murine leukemia (bcr-abl) kinase-carrying leukemic K562 cells. For apoptosis induction or growth arrest, nanomolar concentrations of NSC606985 are sufficient. At such low concentrations, this agent also significantly inhibits the clonogenic activity of hematopoietic progenitors from patients with AML. For apoptosis induction, NSC606985 rapidly induces the proteolytic activation of protein kinase Cδ (PKCδ) with loss of mitochondrial transmembrane potential (ΔΨm) and caspase-3 activation. Cotreatment with rottlerin, a PKCδ-specific inhibitor, completely blocks NSC606985-induced mitochondrial ΔΨm loss and caspase-3 activation, while the inhibition of caspase-3 by z-DEVD-fluoromethyl ketone (Z-DEVD-fmk) only partially attenuates PKCδ activation and apoptosis. These data indicate that NSC606985-induced PKCδ activation is an early event upstream to mitochondrial ΔΨm loss and caspase-3 activation, while activated caspase-3 has an amplifying effect on PKCδ proteolysis. In addition, NSC606985-induced apoptosis by PKCδ also involves caspase-3–independent mechanisms. Taken together, our results suggest that NSC606985 is a potential agent for the treatment of AML. (Blood. 2005;105: 3714-3721)

Introduction

Acute myeloid leukemia (AML), a heterogenous group of hematopoietic malignancies, is the most common variant of acute leukemia occurring in adults. As documented, approximately 11 000 Americans were diagnosed with AML in 2003, and about 75% would ultimately die of this disease.[1] Significant advances in understanding biologic, molecular, and cytogenetic aspects of this malignancy have been achieved in the past 20 years. Meanwhile, substantial progress is also made in the treatment of patients with AML.[2] Especially, the application of *all-trans* retinoic acid, its combination with anthracycline-based chemotherapy, and with the addition of arsenic trioxide[3] make patients with acute promyelocytic leukemia (APL), a unique subtype of AML with specific chromosome translocation t(15;17),[4] become curable as reviewed by Tallmann.[5] Prognosis of other AMLs is also being gradually improved as a result of the use of cytarabine and anthracycline-containing current chemotherapy in combination with advanced supportive care, which enable 75% to 80% of patients with AML to reach clinical remission. Unfortunately, most patients will relapse and live with incurable disease,[6,7] although some of them may be salvaged with expensive stem cell transplantation.[8] Furthermore, the results of intensive chemotherapy still remain disappointing in elderly patients with AML.[9] Therefore, it is imperative to develop novel agents for the treatment of this disease. An appealing alternative approach is to induce cell apoptosis with novel agents,[10] since apoptosis is the mechanism used by metazoans to eliminate deleterious cells and plays a major role in the development, immune system maturation, tissue homeostasis, and aging.[11]

Camptothecin, an alkaloid isolated from the Chinese tree *Camptotheca acuminata*, represents a promising new class of anticancer drugs that target the intranuclear enzyme topoisomerase I (topo-I).[12] Initial clinical studies of camptothecin were halted because of severe and unpredictable adverse effects. Supported by detailed understanding of their mechanism of action and facilitated by chemical manipulations that have amplified their solubility, camptothecins have advanced to the forefront of several areas of therapeutic and developmental chemotherapy.[13] Especially, 2 water-soluble camptothecin analogs were approved by the Food and Drug Administration for clinical application: topotecan as a second-line therapy for ovarian cancer or small-cell lung cancer

From the Department of Pathophysiology, Shanghai Institute of Hematology, Rui-Jin Hospital, Shanghai Second Medical University, Shanghai, China; the Health Science Center, Shanghai Institutes for Biological Sciences and Graduate School, Chinese Academy of Sciences, Shanghai, China; the Department of Hematology, Zhong-Shan Hospital, Fu-Dan University, Shanghai, China; and the Department of Medicine/Endocrinology, Weill Medical College of Cornell University, New York, NY.

Submitted October 19, 2004; accepted December 30, 2004. Prepublished online as *Blood* First Edition Paper, January 25, 2005; DOI 10.1182/blood-2004-10-4011.

Supported in part by National Key Program (973) for Basic Research of China (NO2002CB512805), International Collaborative Items of Ministry of Science and Technology of China (2003DF000038), Science and Technology Commission of Shanghai (grants 02DJ14008, 04DZ14901, and 03XD14016), and 100-Talent Program of Chinese Academy of Sciences.

M-G.S., S-M.G, and K-M.D. contributed equally to this work.

Reprints: Guo-Qiang Chen, No. 280, Chong-Qing South Rd, Shanghai 200025, China; e-mail: chengq@shsmu.edu.cn.

The publication costs of this article were defrayed in part by page charge payment. Therefore, and solely to indicate this fact, this article is hereby marked "advertisement" in accordance with 18 U.S.C. section 1734.

and irinotecan for the treatment of colorectal carcinoma refractory to 5-fluorouracil or as initial therapy in combination with 5-flurouracil for the treatment of metastatic colorectal cancer.[12]

The clinical potentials of camptothecin analogs in the treatment of AML were also investigated. In 1996, Rowinsky et al[14] reported that topotecan administered as a single agent had a significant antileukemic activity in patients with AML. Recently, topotecan was investigated as a salvage and front-line therapy for AML in combination with etoposide, cytarabine, or cyclophosphamide, and some efficacious results were obtained.[15-17] Further development of novel topo-I inhibitors was spurred by the spectrum of potencies of this class of drugs in terms of enzyme inhibition, antiproliferative activity, toxicities, and pharmaceutical properties. For instance, DX-8951f, a water-soluble hexacyclic camptothecin derivative with more potent topo-I–inhibiting action, has been shown to possess better antileukemic activity in severe combined immunodeficient (SCID) mice with AML.[18] Potent preclinical antileukemic activity is also observed for OSI-211, a low-clearance, unilamellar liposomal formulation of a water-soluble camptothecin analog lurtotecan.[19]

In the present study, we report that very low concentrations (nanomolar, nM) of NSC606985, a rarely studied water-soluble camptothecin ester derivative (Figure 1A),[20] can induce leukemic cell apoptosis by proteolytic activation of protein kinase Cδ (PKCδ). By using this system, the relationship among PKCδ, mitochondrial transmembrane potentials ($\Delta\Psi m$), and caspase-3 activation in apoptosis regulation is also evaluated.

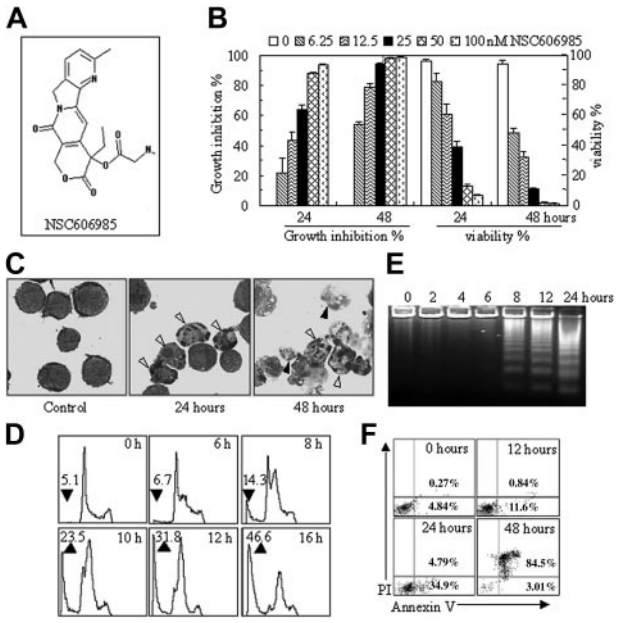

Figure 1. NSC606985 at nanomolar concentrations induces apoptosis in NB4 cells. (A) Chemical structure of NSC606985 (adapted from Rapisarda et al[20]; image reproduced with permission from the American Association for Cancer Research). (B) NB4 cells were treated with NSC606985 for 24 and 48 hours at the indicated concentrations, and growth-inhibiting percentages (left) and viability (right) were measured by trypan-blue exclusion assay. Each column represents the mean + SD of triplicates in an independent experiment. (C) NB4 cells treated with or without 25 nM NSC606985 for the indicated times were collected onto slides by cytospin, stained with Wright stain, and examined under an Olympus BX60 microscope equipped with a 100 ×/1.3 objective lens (Olympus, Tokyo, Japan). Images were acquired through a SPOT RT camera and SPOT software (Diagnostic Instruments, Sterling Heights, MI). Open arrowheads indicate apoptotic cells, and filled arrowheads point to secondary necrotic cells. (D-E) NB4 cells were treated with 25 nM NSC606985 for the indicated times, and analyses of nuclear DNA content distribution (D), DNA fragmentation (E),and annexin-V assay (F) were performed as described in "Patients, materials, and methods." The arrow-pointed numbers in panel D represent the percentage of apoptotic cells, and the values are the mean of triplicates. The numbers in panel F represent the percentage of annexin-V^+/PI^- (lower right quadrant) and annexin-V^+/PI^+ (upper right quadrant) cells. All experiments were repeated 5 times with similar results.

Patients, materials, and methods

Cell culture and treatment

Leukemic cells, including APL cell line NB4 (kindly provided by Dr Michael Lannotte,[21] INSERM u-496, Centre G. Hayem, Hospital Saint-Louis, Paris, France), acute myelomonocytic leukemic U937 cell line, and chronic myeloid leukemic K562 cell line (Cell Bank of Shanghai Institutes for Biological Sciences, Shanghai, China), were cultured in RPMI-1640 medium (Sigma, St Louis, MO) supplemented with 10% heat-inactivated fetal calf serum (FCS; HyClone, Logan, UT) in a 5% CO_2 95% air humidified atmosphere at 37°C. For experiments, cells were seeded at 2 to 5×10^5 cells/mL and incubated with the indicated concentrations of NSC606985 with or without the PKCδ-specific inhibitor rottlerin and caspase-3 inhibitor z-DEVD-fluoromethyl ketone (Z-DEVD-fmk). Etoposide was also used for apoptosis induction in K562 cells. NSC606985 (kindly provided by National Cancer Institute Anticancer Drug Screen standard agent database, Bethesda, MD) was dissolved in double-distilled water as a 25 μM stock solution. Rottlerin (BIOMOL, Plymouth, PA) was prepared in ethanol as 1 mM stock solution and was kept at −80°C. Z-DEVD-fmk (BD Biosciences, San Diego, CA) was dissolved in dimethyl sulfoxide (DMSO) before use. Etoposide (BIOMOL) was also dissolved in DMSO as 20 mM stock solution and kept at −20°C. Cell viability was determined by the trypan-blue exclusion assay, and growth inhibition rate was calculated according to viable cell numbers of treated cells against numbers of untreated cells. For morphologic observation, cells were collected onto slides by cytospin (Shandon, Runcorn, United Kingdom), stained with Wright staining, and examined under light microscope.

Flow cytometric assays for nuclear DNA content distribution, mitochondrial transmembrane potentials, and annexin-V

To assess the distribution of nuclear DNA content, cells were collected, rinsed, and fixed overnight in 70% cold ethanol at −20°C. Then, cells were treated with Tris (tris(hydroxymethyl)aminomethane)–HCl buffer (pH 7.4) supplemented with 1% RNase and stained with 50 μg/mL propidium iodide (PI; Sigma). Cell-cycle distribution was determined by flow cytometry (Beckman Coulter, Miami, FL). All data were collected, stored, and analyzed by Multicycle software (Beckman Coulter). The mitochondrial $\Delta\Psi m$ assay was performed as we described previously.[22] Briefly, about 10^6 cells were rinsed with phosphate-buffered saline (PBS) and incubated with 10 μg/mL rhodamine 123 (Rh123; Sigma) at 37°C for 30 minutes. Subsequently, cells were washed with PBS and stained with 50 μg/mL PI. Fluorescent intensities of Rh123, PI, or both were determined by flow cytometry (Beckman Coulter). Annexin-V assay was performed on a flow cytometry (Beckman Coulter) according to instructions provided by the ApoAlert Annexin-V kit (Clontech, Palo Alto, CA).

DNA gel electrophoresis

Appropriate 10^6 cells were harvested, and pellets were suspended in lysis buffer (0.1 M NaCl, 50 mM Tris-HC1, pH 7.5, 10 mM EDTA (ethylenediaminetetraacetic acid), 0.5% sodium dodecyl sulfate [SDS], 500 μg/mL protease K). After a 30-minute incubation on ice, samples were centrifuged at 14 000*g* for 30 minutes, and cellular DNA was extracted. The samples were electrophoresed in 2% agarose gel at 100 V in 40 mM Tris-acetate buffer (pH 7.4) and visualized by ethidium bromide staining.

Nuclear and cytoplasmic fractionation

Cells (about 1×10^7) were incubated in 400 μL lysis buffer (10 mM HEPES (*N*-2-hydroxyethylpiperazine-*N*′-2-ethanesulfonic acid), 10 mM KCl, 1.5 mM $MgCl_2$, 0.5 mM DTT (dithiothreitol), pH 7.9) with the

supplement of 0.2% Nonidet P-40 (NP-40; [octylphenoxy]polyethoxyethanol) and protease inhibitor cocktail (Sigma) for 1 minute on ice. The lysates were microcentrifuged for 1 minute at 2300*g*. The supernatants were collected for cytoplasmic protein extracts. Then, the pellets were washed with lysis buffer without NP-40 and resuspended in 150 μL extraction buffer (20 mM HEPES, pH 7.9, 420 mM NaCl, 0.5 mM DTT, 0.2 mM EDTA, and 25% glycerol) and incubated for 20 minutes on ice. The samples were centrifuged at 12 000*g* for 10 minutes, and the supernatant was collected as nuclear protein extracts.

Western blots

Cells were washed with PBS and lysed with lysis buffer (62.5 mM Tris-HCl, pH 6.8, 100 mM DTT, 2% SDS, 10% glycerol). Cell lysates were centrifuged at 20 000*g* for 10 minutes at 4°C, and proteins in the supernatants were quantified. Protein extracts were equally loaded to an 8% to 14% SDS–polyacrylamide gel, electrophoresed, and transferred to nitrocellulose membrane (Amersham Bioscience, Buckinghamshire, United Kingdom). The blots were stained with 0.2% Ponceau S red to ensure equal protein loading. After blocking with 5% nonfat milk in PBS, the membranes were probed with anti-PKCδ (1:2000, C-20; Santa Cruz Biotech, Santa Cruz, CA), anticleaved caspase-3 (1:1000; Cell Signaling, Beverly, MA), and poly(ADP [adenosine diphosphate]–ribose) polymerase (PARP; 1:500, F2; Santa Cruz Biotech), followed by horseradish peroxidase (HRP)–linked secondary antibodies (Cell Signaling). The signals were detected by chemiluminescence phototope-HRP kit (Cell Signaling) according to manufacturer's instructions. As necessary, blots were stripped and reprobed with anti–β-actin antibody (Oncogene, Fremont, CA) as an internal control. All experiments were repeated 3 times with the similar results.

Patients, erythroid burst-forming unit (BFU-E), and granulocyte-macrophage colony-forming unit (CFU-GM) assay

Bone marrow (BM) was obtained, with informed consent, from 4 patients with AML, including 2 cases of M3, 1 case of M2, and 1 case of M5 AML according to French-American-British classification. Mononuclear cells were aspirated by Ficoll-Paque liquid and suspended in Iscoves modified Dulbecco medium (IMDM; Gibco BRL, Gaithersburg, MD). Viable cells were counted by trypan-blue exclusion, and then they were diluted to a concentration of 2×10^5 cells/mL. Cells were diluted 1:10 in IMDM containing 10% FCS (HyClone, Logan, UT) with or without 25 nM and 50 nM NSC606985 and were plated in 24-well cell culture plates with Methocult GF H4434 (Stem Cell Technologies, Vancouver, BC). Colonies (> 40 cells) were counted after 14 days of incubation at 37°C with 5% CO_2 and humidified air. These experiments were approved by the Clinical Investigational Reviewing Board of Shanghai Second Medical University, Shanghai, China.

Statistical analysis

The significance of the difference between groups was determined by the Student *t* test.

Results

NSC606985 at nanomolar concentration induces apoptosis in acute promyelocytic leukemic cell line

In APL cell line NB4 cells, NSC606985 inhibited cell growth in a time- and concentration-dependent manner (Figure 1B, left), which paralleled to the reduced cell viability (Figure 1B, right). This inhibitory effect was observed at nanomolar concentrations. At 48 hours of treatment, 6.25 nM NSC606985 produced 48.2% ± 2.8% cell death, and 50 nM and 100 nM NSC606985 almost caused all cells to die (Figure 1B, right). Further evidence supported that NSC606985 induced cell death by way of apoptosis. NB4 cells treated with NSC606985 presented profound morphologic changes that were characteristics of apoptosis, such as chromatin condensation and nuclear fragmentation with intact cell membrane (Figure 1C). Analysis of nuclear DNA distribution on flow cytometry showed that NSC606985 induced a time-dependent increase in hypoploid cells (also called sub-G_1 cells) as a result of the degradation and subsequent leakage of nuclear DNA from cells, an important indication of cells becoming apoptotic (Figure 1D).[23] In agreement with this, treatment with NSC606985 in NB4 cells also induced apoptosis-specific DNA-laddering fragmentation on the agarose gel electrophoresis (Figure 1E). Furthermore, annexin V/PI double staining–based flow cytometry analysis, the most sensitive and the most specific test for determining apoptotic cells in suspension culture,[24] showed that at early phase after 25 nM NSC606985 treatment, annexin-V^+/PI^- cells were present (Figure 1F). Subsequently, cells underwent secondary necrosis, as evidenced by increased annexin-V^+/PI^+ cells (Figure 1F, 48 hours) and necrotic cell–like morphology (Figure 1C).

NSC606985 produces differential effects in different leukemic cells

The effect of NSC606985 on cell apoptosis was further examined in 2 other myeloid leukemic cells, U937, a cell line from acute myelomonocytic leukemia, and K562, a cell line from t(9,22)–carrying chronic myeloid leukemia. Like that in NB4 cells, NSC606985 inhibited the cell growth in both U937 and K562 cells in a time- and concentration-dependent manner (Figure 2A-B). Although 6.25 nM NSC606985 was sufficient for potent proliferation-inhibitory effect in K562 cells (Figure 2D), the compound failed to induce apoptosis in the cell line, even at a high concentration (200 nM), as determined by cell morphologic criteria (Figure 2C), DNA fragmentation (Figure 2D), annexin-V/PI assay, and cellular DNA content distribution assay (data not shown). As described by previous reports,[25,26] etoposide at 100 μM could induce apoptosis in K562 cells (Figure 2C-D), indicating that the resistance of K562 cells to NSC606985-induced apoptosis was not due to clonal selection.

In U937 cells, nanomolar concentration of NSC606985 also effectively induced apoptosis (Figure 2C-E), although the sensitivity of the cells to NSC606985-induced apoptosis was lower than that of NB4 cells. Under the treatment with NSC606985 at 50-nM concentration for 24 hours, only 21.63% ± 1.64% of U937 cells underwent apoptosis compared with 76.09% ± 5.40% of NB4 cells ($P < .001$), as assessed by annexin-V analysis. Because of the different sensitivity to NSC606985, NB4 cells and U937 cells were treated respectively with 25 nM and 50 nM NSC606985 for all following experiments, aiming to elucidate the mechanisms of the agent-induced apoptosis.

NSC606985 at apoptosis-inducing concentrations induces proteolytic activation of PKCδ with mitochondrial transmembrane potential collapse and caspase-3 activation

To elucidate the mechanisms of NSC606985-induced apoptosis, we first determined the effects of NSC606985 on mitochondrial $\Delta\Psi m$ by double staining of PI and Rh123, a lipophilic cation that is taken up by mitochondria in proportion to the $\Delta\Psi m$.[27] As depicted in Figure 3A, untreated living cells were strongly stained by Rh123 with negative PI. When NB4 cells were treated with 25 nM NSC606985 for 12 hours (Figure 3A, top) or U937 cells treated with 50 nM NSC606985 for 36 hours (Figure 3A, bottom), PI-negative but weaker Rh123-stained cells began to appear and subsequently increased. Following mitochondrial $\Delta\Psi m$ collapse,

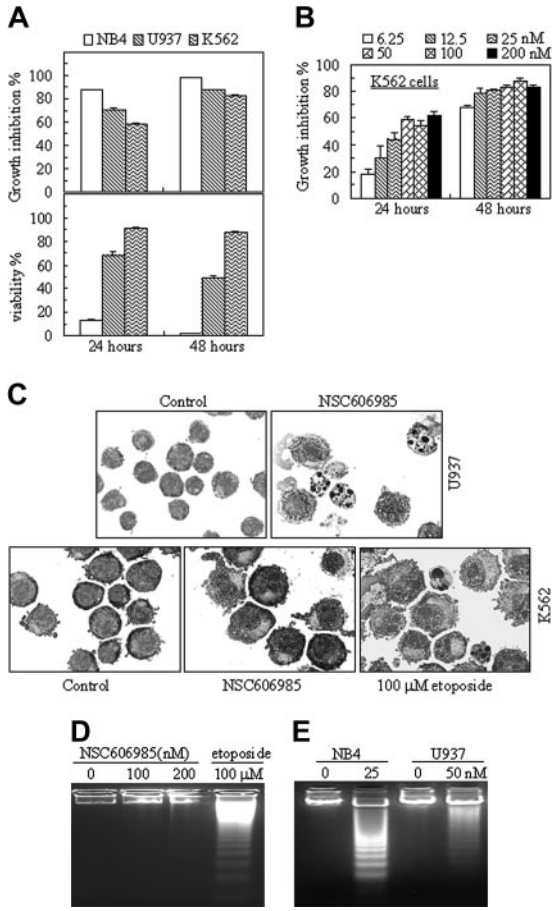

Figure 2. Three leukemic cell lines show different sensitivity to NSC606985-induced apoptosis. (A) NB4, U937, and K562 cells were treated with 50 nM NSC606985 for 24 and 48 hours. Growth-inhibiting rate (top) and cell viability (bottom) were determined. The values are the mean + SD of a triplicate experiment. (B) K562 cells were incubated with the indicated concentrations of NSC606985 for 24 and 48 hours, and the growth inhibition rates were determined. The values are the mean + SD of a triplicate experiment. (C) U937 (top row) and K562 cells (bottom row) were treated with or without 50 nM and 100 nM NSC606985, respectively, for 48 hours. Cytomorphology was examined with Wright staining. Images were viewed using an Olympus BX60 microscope equipped with a 100 ×/1.3 objective lens, and were acquired through a SPOT RT camera and SPOT software. For K562 cells, the treatment with etoposide at 100 μM for 24 hours was used as positive control. (D) K562 cells were incubated with the indicated concentrations (nM) of NSC606985 or with 100 μM etoposide for 48 hours. DNA samples from these treated cells were electrophoresed in a 2% agarose gel. (E) NB4 and U937 cells were treated with NSC606985 at the indicated concentrations for 48 hours, and DNA samples from the cells were electrophoresed in a 2% agarose gel. All experiments were repeated 4 times with similar results.

caspase-3 was also activated by NSC606985 as determined by Western blot analysis using specific antibody against active caspase-3 (Figure 3B). Parallel to this, PARP, a substrate of casapse-3, was degraded after NSC606985 treatment (Figure 3B). However, NSC606985 but not etoposide failed to induce mitochondrial ΔΨm collapse (data not shown) and caspase-3 activation/PARP degradation in K562 cells that are insensitive to the agent-induced apoptosis (Figure 3C).

NSC606985 at apoptosis-inducing concentrations also induced a rapid proteolytic cleavage of PKCδ into a 41-kDa catalytic fragment that persistently activates the kinase,[28-30] in NB4 cells and U937 cells (Figure 4A) but not in K562 cells (Figure 3C). This proteolytic effect was clearly observed at 12 and 24 hours after the treatment with NSC606985 in NB4 cells and U937 cells (Figure 4A), respectively. The similar results could also be seen in etoposide-treated K562 cells (Figure 3C). Moreover, the cleavage

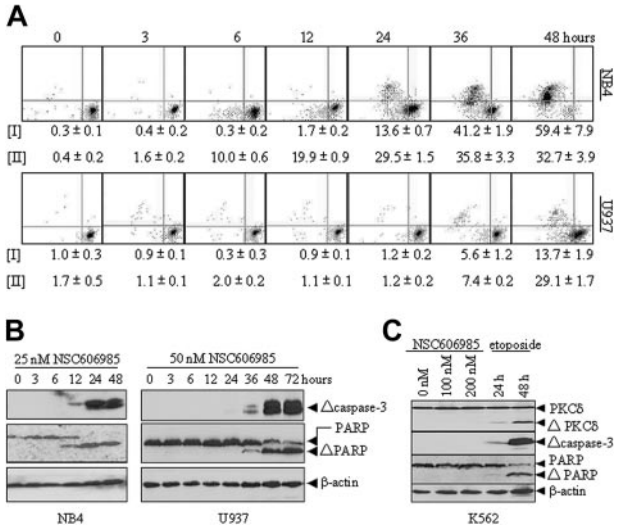

Figure 3. NSC606985 induces mitochondrial transmembrane potential loss and caspase-3 activation in NB4 and U937 cells but not in K562 cells. (A-B) NB4 and U937 cells were treated with or without 25 nM and 50 nM NSC606985, respectively, for the indicated times, the mitochondrial ΔΨm (A) was measured on flow cytometry, and the active (Δ) caspase-3 and PARP proteins (B) were detected by Western blots. For the mitochondrial ΔΨm (A), abscissa and vertical axiles represent the fluorescent intensities of Rh123 and PI, respectively. The numbers below panels represent the mean ± SD of a triplicate experiment. [I] and [II] represent, respectively, percentage of $Rh123^{low}/PI^{+}$ and $Rh123^{low}/PI^{-}$ cells. (C) K562 cells were treated with or without NSC606985 at the indicated concentrations for 48 hours. The treatment with 100 μM etoposide for the shown hours was used as a positive control. PKCδ, Δcaspase-3, and PARP proteins were detected by Western blots. For Western blots, β-actin was used as an internal control. All experiments were repeated 3 times with similar results.

of PKCδ was observed in both cytoplasm and nuclei of NB4 and U937 cells (Figure 4B). PKCδ was present in both cytoplasm and the nucleus of untreated U937 cells, while it was undetectable in the cytoplasm of untreated NB4 cells. It appears that the treatment with NSC606985 increased the level of cytoplasmic PKCδ in NB4 cells (Figure 4B).

NSC606985-induced mitochondrial transmembrane potential loss, caspase-3 activation, and apoptosis are blocked by a PKCδ-specific inhibitor

To determine the role of proteolytic activation of PKCδ in NSC606985-induced apoptosis, we treated NB4 and U937 cells with NSC606985 in the presence or absence of rottlerin (1 μM), a specific PKCδ inhibitor.[31] As showed in Figure 5A, rottlerin significantly inhibited NSC606985-induced proteolytic cleavage of

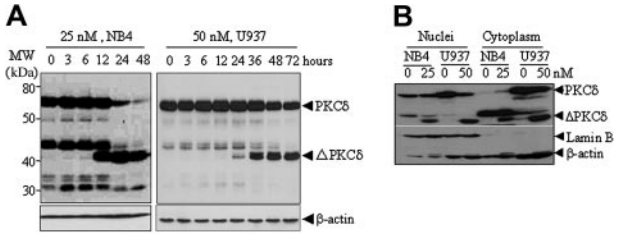

Figure 4. NSC606985 induces proteolytic cleavage of PKCδ proteins in NB4 and U937 cells. (A) NB4 and U937 cells were treated with or without 25 nM and 50 nM NSC606985, respectively, for the indicated times. PKCδ proteins were detected by Western blots with β-actin as an internal control. Molecular weights (MWs) of standard protein markers were indicated. ΔPKCδ indicates cleaved 41-kDa catalytic fragment of PKCδ proteins. (B) NB4 cells were treated with 25 nM NSC606985 for 12 hours, and U937 cells were treated with 50 nM NSC606985 for 36 hours. Nuclear and cytoplasmic proteins were extracted and subjected to Western blotting for the detection of PKCδ proteins. Lamin B was used as a nuclear protein control.

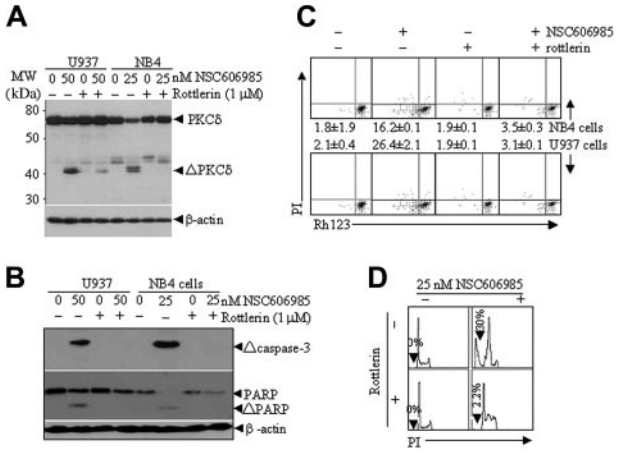

Figure 5. Rottlerin inhibits NSC606985-induced caspase-3 activation, mitochondrial transmembrane potential loss, and apoptosis. (A-B) After preincubated with 1 μM rottlerin for 1 hour, NB4 and U937 cells were treated with 25 nM and 50 nM NSC606985 for 12 and 36 hours, respectively. PKCδ (A), the active (Δ) caspase-3, and PARP proteins (B) were determined by Western blots. ΔPKCδ indicates cleaved 41-kDa catalytic fragment of PKCδ proteins. (C) NB4 cells (top row) and U937 cells (bottom row) were treated as described for panels A and B. The mitochondrial ΔΨm was measured on flow cytometry. The numbers (percentage of $Rh123^{low}$ cells) represent the mean ± SD of a triplicate experiment. (D) NB4 cells were treated as described for panels A and B, and the histograms of nuclear DNA distribution are presented. The number in each panel indicates the percentage of sub-G_1 (Ap) cells. Similar results were obtained in U937 cells (data not shown). All experiments were repeated 3 times with similar results.

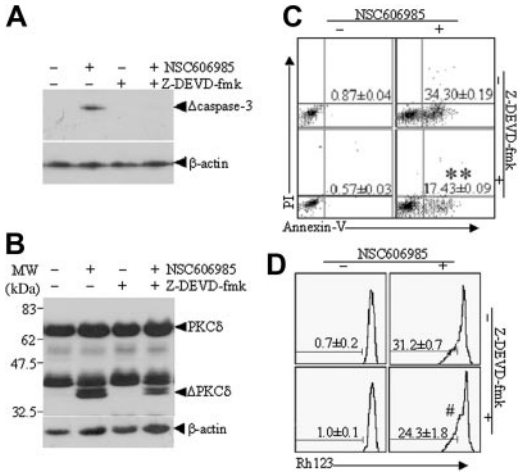

Figure 6. Caspase-3 inhibitor, Z-DEVD-fmk, partly inhibits NSC606985-induced proteolysis of PKCδ proteins and apoptosis in NB4 cells. NB4 cells were preincubated with 40 μM Z-DEVD-fmk for 1 hour and then treated with or without 25 nM NSC606985 for 12 hours. The active caspase-3 (A) and PKCδ proteins (B) were detected by Western blots. ΔPKCδ indicates cleaved 41-kDa fragment of PKCδ proteins. The annexin V (C) and mitochondrial ΔΨm (D) were measured on flow cytometry. The numbers in panels C and D indicate the percentages of annexin-V^+/PI^- cells and low ΔΨm cells, respectively. The numbers are the mean ± SD of a triplicate experiment. $^{**}P < .01$ and $^{\#}P > .05$ by the Student *t* test, compared with NSC606985 treatment alone.

PKCδ. In agreement with this effect, the inhibitor also antagonized NSC606985-induced caspase-3 activation, PARP degradation (Figure 5B) and mitochondrial ΔΨm collapse (Figure 5C). Most importantly, rottlerin completely blocked NSC606985-induced apoptosis in both NB4 cells (Figure 5D) and U937 cells (data not shown). These results strongly indicated that NSC606985-induced PKCδ activation was an early event upstream to the mitochondrial ΔΨm collapse and caspase-3 activation and was essential for NSC606985-induced apoptosis in NB4 and U937 cells.

NSC606985-induced PKCδ activation and apoptosis, but not mitochondrial transmembrane potential collapse, are partially antagonized by a caspase-3 inhibitor

To understand the role of caspase-3 and possible relationship between caspase-3 activation and PKCδ cleavage in NSC606985-induced apoptosis, NB4 cells were treated with NSC606985 in the presence or absence of the cell-permeable caspase-3 inhibitor Z-DEVD-fmk. As showed in Figure 6, Z-DEVD-fmk completely blocked the NSC606985-induced caspase-3 activation (Figure 6A) but only partially inhibited NSC606985-induced proteolytic cleavage of PKCδ (Figure 6B) and apoptosis (Figure 6C). Treatment of NB4 cells with 25 nM NSC606985 alone for 12 hours greatly induced cell apoptosis, which was significantly attenuated by the addition of Z-DEVD-fmk (40 μM) 1 hour before NSC606985 treatment, as assessed by the percentage of annexin V^+/PI^- cells ($P < .01$, compared with NSC606985 treatment alone; Figure 6C). However, the addition of Z-DEVD-fmk did not significantly affect NSC606985-induced mitochondrial ΔΨm collapse ($P > .05$, compared with NSC606985 treatment alone; Figure 6D).

NSC606985 inhibits the formation of CFU-GM and BFU-E of AML patients

Finally, we determined the effects of NSC606985 on the clonogenic activity of fresh BM cells from 4 patients with AML using CFU-GM and BFU-E assays. As shown in Figure 7A-B, treatment with 25 nM and 50 nM NSC606985 significantly inhibited CFU-GM formation and resulted in a 100% inhibition in case 3 and case 4. Except for case 2 and case 4 patients whose BM cells did

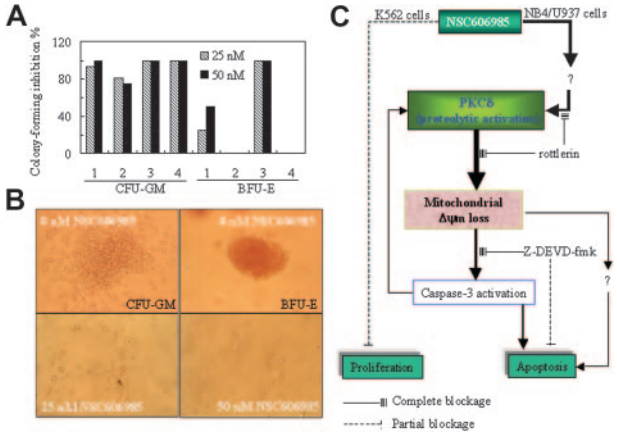

Figure 7. NSC606985 inhibits the formation of CFU-GM and BFU-E of bone marrow cells from patients with AML and a sketch of mechanisms of NSC606985 action in leukemic cells. (A) BM mononuclear cells were cultured for colony assay as described in "Patients, materials, and methods." In cases 1 to 4, the number of colonies per well in vehicle control was 33, 16, 40, and 20, respectively, for CFU-GMs. For BFU-E, the number of colonies per well in vehicle control was 37 and 20, respectively, while BM cells from case 2 and case 4 patients did not form BFU-Es. The values represent the inhibition % of colony formation compared with control. (B) Representative images of CFU-GMs and BFU-Es for the case-3 patient. Images were visualized with an Olympus IMT microscope equipped with a 40 ×/0.5 numerical aperture objective lens (Olympus), and were captured through a SPOT RT camera and SPOT software. (C) An illustration of the potential mechanisms of NSC606985 action in leukemic cells. NSC606985 at nanomolar concentrations activates PKCδ that leads to mitochondrial ΔΨm loss and activation of caspase-3, resulting in apoptosis. These events were completely blocked by PKCδ-specific inhibitor rottlerin. However, caspase-3 inhibitor Z-DEVD-fmk only partially blocks NSC606985-induced apoptosis, indicating that caspase-3–independent mechanisms are also involved in the event. The activated caspase-3 has a positive feedback to proteolytic activation of PKCδ. The inhibition of cell proliferation by NSC606985 may involve independent mechanisms from cell apoptosis. Solid lines indicate complete blockage; dashed lines, partial blockage.

not form BFU-E in untreated condition, the BFU-E formation in2 other patients was also significantly inhibited by NSC606985.

Discussion

Here, we reported that a camptothecin analog NSC606985 produced a time- and dose-dependent induction of cell apoptosis in leukemic NB4 and U937 cells, as demonstrated by cell morphologic features, sub-G_1 cell, DNA-laddering fragmentation, and annexin V^+/PI^- cell analysis. In K562 cells, NSC606985 possessed more potent inhibitory activity on cell proliferation but failed to induce cell apoptosis. Both apoptosis-inducing and proliferation-inhibiting effects were observed at nanomolar concentrations of the agent. Furthermore, apoptosis-inducing or proliferation-inhibiting concentrations of NSC606985 significantly inhibited the clonogenic activity of fresh hematopoietic progenitors from patients with AML. These results indicated that NSC606985 might be a potential therapeutic remedy for the treatment of leukemia.

It has been well known that a complex cellular signaling network contributes to the regulation of apoptosis. In most cases, a central player in the execution of apoptosis is aspartic acid–directed cysteine proteases called caspases, which are activated by the cell surface death receptor pathway and the mitochondria-initiated pathway,[32] the latter inducing the release of proteins such as cytochrome c from the intermembrane space of $\Delta\Psi$m-collapsed mitochondria.[33] Here, we showed that NSC606985-induced apoptosis paralleled to the mitochondrial $\Delta\Psi$m loss and caspase-3 activation, but caspase-3–specific inhibitor only partially attenuated NSC606985-induced apoptosis, indicating that casapse-3 pathway partially contributed to leukemic cell apoptosis induced by NSC606985. PKCδ, a ubiquitously expressed member of the novel PKC family, is activated by translocation, tyrosine phosphorylation, or proteolytic cleavage into 41-kDa catalytically active fragment. The isoenzyme enigmatically presents the multifunctional properties and is implicated in the regulation of a variety of cellular processes, including secretion, cell cycle progression, apoptosis, differentiation, and tumor development.[34-36] In 1994, Trubiani et al[37] reported for the first time that treatment with dexamethasone in thymocytes resulted in a redistribution of PKC to the nucleus and cell apoptosis, indicating a linkage between PKC activation and cell apoptosis. From then on, increasing data supported a direct link between PKCδ activation and cell apoptosis induced by diverse agents such as etoposide,[30] ara-C,[38] taxol,[31] and many others.[39-41] However, conflicting results have been reported, and the functional significance of PKCδ in cell apoptosis has not been clearly defined, as reviewed by Jackson and Foster.[36] In the present study, we show that, like that seen in etoposide-treated K562 cells, NSC606985 rapidly induced proteolytic activation of PKCδ and subsequently cell apoptosis in NB4 and U937 cells but not in K562 cells. The PKCδ-specific inhibitor rottlerin completely attenuated NSC606985-induced apoptosis, suggesting that PKCδ played a critical role in NSC606985-induced apoptosis, and the NSC606985-induced PKCδ activation was directly linked to NSC606985-induced cell apoptosis (Figure 7C).

It was proposed that PKCδ proteolytic activation was completely dependent on caspase-3, based on the observations that inhibition of caspase-3 activity blocked PKCδ cleavage and apoptosis induced by ultraviolet radiation,[42] oxidative stress,[43,44] DNA damage,[45] aging neutrophil[31] as well as other inducers.[32,46] Here, we demonstrated that the blockage of PKCδ activity by rottlerin completely blocked NSC606985-induced mitochondrial $\Delta\Psi$m loss and caspase-3 activation, indicating that PKCδ activation was an event upstream to mitochondrial $\Delta\Psi$m loss and caspase-3 activation. This result was consistent with reports that PKCδ directly interacts with mitochondria and alters mitochondrial function for apoptosis induction,[47] presumably mediated through amplifying ceramide formation and the ceramide-mediated mitochondrial amplification loop.[48] Furthermore, we showed that inhibition of caspase-3 activity by Z-DEVD-fmk only partially attenuated PKCδ cleavage and apoptosis without significant alteration in NSC606985-induced mitochondrial $\Delta\Psi$m loss, supporting the amplifying effect of activated caspase-3 on PKCδ cleavage. More important, these results also proposed that in addition to caspase-3, PKCδ-mediated apoptosis also involved caspase-3–independent mechanisms that remain to be addressed (Figure 7C). It is possibly associated with some potential downstream carriers of PKCδ action in the induction of apoptosis such as DNA-dependent protein kinase,[49] p38 mitogen-activated protein kinase,[50] Rad9,[51] and p73β (a structural and functional homolog of the p53 tumor suppressor[52]).

It has previously been reported that subcellular localization of PKCδ affects its apoptosis-inducing effect. DeVries et al[53] showed that the import of PKCδ into the nucleus was required for the initiation of etoposide-induced apoptosis, while the attachment of PKCδ to membrane and translocation to the Golgi complex was required for the ultraviolet- and ceramide-induced apoptosis, respectively.[54,55] Here, we showed that NSC606985-induced PKCδ cleavage simultaneously occurred in the cytoplasm and nuclei of both NB4 and U937 cells, although PKCδ was differentially distributed within these cells. Unlike untreated U937 cells in which PKCδ was present in the cytoplasm and nuclei, NB4 cells had undetectable level of cytoplasmic PKCδ. Treatment with NSC606985 increases the levels of cytoplasmic PKCδ in NB4 cells. Whether differential subcellular distribution of PKCδ is related to the cell sensitivity to NSC606985-induced apoptosis and whether the NSC606985-induced increase in cytoplasmic PKCδ is translocated from other subcellular compartments remain to be determined. It should be pointed out that a higher level of an anti-PKCδ antibody cross-reactive fragment (about 45 kDa), which existed mainly in the cytoplasm and also down-regulated by NSC606985 treatment, could be clearly seen in NB4 cells, while such a protein was weaker in U937 cells (Figure 4). It remains to be clarified whether the fragment may make NB4 cells more susceptible to NSC606985.

Finally, the cause leading to the difference of effects of NSC606985 on NB4 and U937 cells and on K562 cells remains to be investigated. It has been proposed that the strong resistance of K562 cells to apoptosis induction is related to bcr-abl tyrosine kinase, generated by specific chromosome translocation t(9;22).[56] Thus, we speculated that the fusion tyrosine kinase also contribute to the failure of K562 cells to NSC606985-induced apoptosis. However, K562 cells were still extremely resistant to NSC606985-induced apoptosis in the presence of STI571 (data not shown), a specific tyrosine kinase inhibitor,[57] proposing that the resistance of K562 cells to NSC606985-induced apoptosis was independent of the constant tyrosine-kinase activity in these cells, which is consistent with the recent finding by Bueno-da-Silva et al.[58]

In summary, the present study demonstrates that NSC606985 at nanomolar concentrations effectively induces leukemic cell apoptosis, decreases cell proliferation, and inhibits the clonogenic activity

of hematopoietic progenitor cells from leukemia patients. The NSC606985-induced apoptosis is mainly mediated through the proteolytic activation of PKCδ that leads to caspase-3 activation and mitochondrial $\Delta\Psi$m loss. These results strongly suggest that NSC606985 is a potential new agent for the treatment of leukemia and deserves further preclinical and clinical studies.

References

1. Iovino CS, Camacho LH. Acute myeloid leukemia: a classification and treatment update. Clin J Oncol Nurs. 2003;7:535-540.
2. Winton EF, Langston AA. Update in acute leukemia 2003: a risk adapted approach to acute myeloblastic leukemia in adults. Semin Oncol. 2004;31:80-86.
3. Chen GQ, Shi XG, Tang W, et al. Use of arsenic trioxide (As_2O_3) in the treatment of acute promyelocytic leukemia (APL), I: As_2O_3 exerts dose-dependent dual effects on APL cells. Blood. 1997; 89:3345-3353.
4. Puccetti E, Ruthardt M. Acute promyelocytic leukemia: PML/RARalpha and the leukemic stem cell. Leukemia. 2004;18:1169-1175.
5. Tallmann MS. Curative therapeutic approaches to APL. Ann Hematol. 2004;83:S81-82.
6. Kimby E, Nygren P, Glimelius B, SBU-group. A systematic overview of chemotherapy effects in acute myeloid leukaemia. Acta Oncol. 2001;40: 231-252.
7. Voliotis D, Diehl V. Challenges in treating hematologic malignancies. Semin Oncol. 2002;29:30-39.
8. Frankel AE, Baer MR, Hogge DE, Stuart RK. Immunotherapy of acute myeloid leukemia. Curr Pharm Biotechnol. 2001;2:209-215.
9. Hamblin TJ. Disappointments in treating acute leukemia in the elderly. N Engl J Med. 1995;332: 1712-1713.
10. Parmar S, Rundhaugen LM, Boehlke L, et al. Phase II trial of arsenic trioxide in relapsed and refractory acute myeloid leukemia, secondary leukemia and/or newly diagnosed patients at least 65 years old. Leuk Res. 2004;28:909-919.
11. Sun SY, Hail N Jr, Lotan R. Apoptosis as a novel target for cancer chemoprevention. J Natl Cancer Inst. 2004;96:662-672.
12. Bomgaars L, Berg SL, Blaney SM. The development of camptothecin analogs in childhood cancers. Oncologist. 2001;6:506-516.
13. Pizzolato JF, Saltz LB. The camptothecins. Lancet. 2003;361:2235-2242.
14. Rowinsky EK, Kaufmann SH, Baker SD, et al. A phase I pharmacological study of topotecan infused over 30 mins for five days in patients with refractory acute leukemia. Clin Cancer Res. 1996;2:1921-1930.
15. Weihrauch MR, Staib P, Seiberlich B, Hoffmann M, Diehl V, Tesch H. Phase I/II clinical study of topotecan and cytarabine in patients with myelodysplastic syndrome, chronic myelomonocytic leukemia and acute myeloid leukemia. Leuk Lymphoma. 2004;45:699-704.
16. Bolanos-Meade J, Guo C, Gojo I, Karp JE. A phase II study of timed sequential therapy of acute myelogenous leukemia (AML) for patients over the age of 60: two cycle timed sequential therapy with topotecan, ara-C and mitoxantrone in adults with poor-risk AML. Leuk Res. 2004;28: 571-577.
17. Giles FJ, Cortes JE, Kantarjian HM, O'Brien SM, Estey E, Beran M. A fludarabine, topotecan, and cytarabine regimen is active in patients with refractory acute myelogenous leukemia. Leuk Res. 2004;28:353-357.
18. Nomoto T, Nishio K, Ishida T, Mori M, Saijo N. Characterization of a human small-cell lung cancer cell line resistant to a new water-soluble camptothecin derivative DX-8951f. Jpn J Cancer Res. 1998;89:1179-1186.
19. Tomkinson B, Bendele R, Giles FJ, et al. OSI-211, a novel liposomal topoisomerase I inhibitor, is active in SCID mouse models of human AML and ALL. Leuk Res. 2003;27:1039-1050.
20. Rapisarda A, Uranchimeg B, Scudiero DA, et al. Identification of small molecule inhibitors of hypoxia-inducible factor 1 transcriptional activation pathway. Cancer Res. 2002;62:4316-4324.
21. Lanotte M, Martin-Thouvenin V, Najman S, Balerini P, Valensi F, Berger R. NB4, a maturation inducible cell line with t(15;17) marker isolated from a human acute promyelocytic leukemia(M3). Blood. 1991;77:1081-1086.
22. Zhu XH, Shen YL, Jing YK, et al. Apoptosis and growth inhibition in malignant lymphocytes after treatment with arsenic trioxide at clinically achievable concentrations. J Natl Cancer Inst. 1999;91: 743-745.
23. Nicoletti I, Migliorati G., Pagliacci MC, Grignani F, Riccardi C. A rapid and simple method for measuring thymocyte apoptosis by propidium iodide staining and flow cytometry. J Immunol Methods. 1991;139:271-279.
24. Overbeeke R, Steffens-Nakken H, Vermes I, Reutelingsperger C, Haanen C. Early features of apoptosis detected by four different flow cytometry assays. Apoptosis. 1998;3:115-121.
25. Ritke MK, Rusnak JM, Lazo JS, et al. Differential induction of etoposide-mediated apoptosis in human leukemia HL-60 and K562 cells. Mol Pharmacol. 1994;46:605-611.
26. Martins LM, Mesner PW, Kottke TJ, et al. Comparison of caspase activation and subcellular localization in HL-60 and K562 cells undergoing etoposide-induced apoptosis. Blood. 1997;90: 4283-4296.
27. Kroemer G, Zamzami N, Susin SA. Mitochondrial control of apoptosis. Immunol Today. 1997;18:44-51.
28. Shin SY, Kim CG, Ko J, et al. Transcriptional and post-transcriptional regulation of the PKC delta gene by etoposide in L1210 murine leukemia cells: implication of PKC delta autoregulation. J Mol Biol. 2004;340:681-693.
29. Khwaja A, Tatton L. Caspase-mediated proteolysis and activation of protein kinase Cδ play a central role in neutrophil apoptosis. Blood. 1999;94: 291-301.
30. Reyland ME, Anderson SM, Matassa AA, Barzen KA, Quissell DO. Protein kinase C delta is essential for etoposide-induced apoptosis in salivary gland acinar cells. J Biol Chem. 1999;274:19115-19123.
31. Matassa AA, Carpenter L, Biden TJ, Humphries MJ, Reyland ME. PKCdelta is required for mitochondria-dependent apoptosis in salivary epithelial cells. J Biol Chem. 2001;276:29719-29728.
32. Boatright KM, Salvesen GS. Mechanisms of caspase activation. Curr Opin Cell Biol. 2003;15: 725-731.
33. Henry-Mowatt J, Dive C, Martinou JC, James D. Role of mitochondrial membrane permeabilization in apoptosis and cancer. Oncogene. 2004;23: 2850-2860.
34. Yuan LW, Soh JW, Weinstein IB. Inhibition of histone acetyltransferase function of p300 by PKCδ. Biochim Biophys Acta. 2002;1592:205-211.
35. Zhao KW, Li X, Zhao Q, et al. Protein kinase Cδ mediates retinoic acid and phorbol myristate acetate-induced phospholipid scramblase 1 gene expression: its role in leukemic cell differentiation. Blood. 2004;104:3731-3738.
36. Jackson DN, Foster DA. The enigmatic protein kinase Cdelta: complex roles in cell proliferation and survival. FASEB J. 2004;18:627-636.
37. Trubiani O, Borgatti P, Di Primio R. Protein kinase C modulation in apoptotic rat thymocytes: an ultrastructural analysis. Histochemistry. 1994;102: 311-316.
38. Emoto Y, Kisaki H, Manome Y, Kharbanda S, Kufe D. Activation of protein kinase Cδ in human myeloid leukemia cells treated with 1-beta-D-arabinofuranosylcytosine. Blood. 1996;87:1990-1996.
39. Meinhardt G, Roth J, Totok G, Auner H, Emmerich B, Hass R. Signaling defect in the activation of caspase-3 and PKCd in human TUR leukemia cells is associated with resistance to apoptosis. Exp Cell Res. 1999;247:534-542.
40. Blass M, Kronfeld I, Kazimirsky G, Blumberg PM, Brodie C. Tyrosine phosphorylation of protein kinase Cdelta is essential for its apoptotic effect in response to etoposide. Mol Cell Biol. 2002;22: 182-195.
41. Ringshausen I, Schneller F, Bogner C, et al. Constitutively activated phosphatidylinositol-3 kinase is involved in the defect of apoptosis in B-CLL: association with protein kinase Cδ. Blood. 2002; 100:3741-3748.
42. Denning MF, Wang Y, Nickoloff BJ, Wrone-Smith T. Protein kinase Cdelta is activated by caspase-dependent proteolysis during ultraviolet radiation-induced apoptosis of human keratinocytes. J Biol Chem. 1998;273:29995-30002.
43. Kanthasamy AG, Kitazawa M, Kanthasamy A, Anantharam V. Role of proteolytic activation of protein kinase Cdelta in oxidative stress-induced apoptosis. Antioxid Redox Signal. 2003;5:609-620.
44. Anantharam V, Kitazawa M, Wagner J, Kaul S, Kanthasamy AG. Caspase-3-dependent proteolytic cleavage of protein kinase Cdelta is essential for oxidative stress-mediated dopaminergic cell death after exposure to methylcyclopentadienyl manganese tricarbonyl. J Neurosci. 2002;22: 1738-1751.
45. Basu A. Involvement of protein kinase C-delta in DNA damage-induced apoptosis. J Cell Mol Med. 2003;7:341-350.
46. Kitazawa M, Anantharam V, Kanthasamy A, Kanthasamy AG. Dieldrin promotes proteolytic cleavage of PARP and apoptosis in dopaminergic cells: protective effect of mitochondrial anti-apoptotic protein Bcl-2. Neurotoxicology. 2004;25: 589-598.
47. Li L, Lorenzo PS, Bogi K, Blumberg PM, Yuspa SH. Protein kinase Cdelta targets mitochondria, alters mitochondrial membrane potential, and induces apoptosis in normal and neoplastic keratinocytes when overexpressed by an adenoviral vector. Mol Cell Biol. 1999;19:8547-8558.
48. Sumitomo M, Ohba M, Asakuma J, et al. Protein kinase Cdelta amplifies ceramide formation via mitochondrial signaling in prostate cancer cells. J Clin Invest. 2002;109:827-836.
49. Bharti A, Kraeft SK, Gounder M, et al. Inactivation of DNA-dependent protein kinase by protein kinase Cdelta: implications for apoptosis. Mol Cell Biol. 1998;18:6719-6728.
50. Efimova T, Broome AM, Eckert RL. Protein kinase Cdelta regulates keratinocyte death and survival by regulating activity and subcellular localization of a p38delta-extracellular signal-regulated kinase 1/2 complex. Mol Cell Biol. 2004;24:8167-8183.
51. Yoshida K, Wang HG, Miki Y, Kufe D. Protein kinase Cdelta is responsible for constitutive and DNA damage-induced phosphorylation of Rad9. EMBO J. 2003;22:1431-1441.

52. Ren J, Datta R, Shioya H, et al. p73beta is regulated by protein kinase Cdelta catalytic fragment generated in the apoptotic response to DNA damage. J Biol Chem. 2002;277:33758-33765.

53. DeVries TA, Neville MC, Reyland ME. Nuclear import of PKCd is required for apoptosis: identification of a novel nuclear import sequence. EMBO J. 2002;21:6050-6060.

54. Chen N, Ma W, Huang C, Dong Z. Translocation of protein kinase Cepsilon and protein kinase Cdelta to membrane is required for ultraviolet B-induced activation of mitogen-activated protein kinases and apoptosis. J Biol Chem. 1999;274:15389-15394.

55. Kajimoto T, Shirai Y, Sakai N, et al. Ceramide-induced apoptosis by translocation, phosphorylation, and activation of protein kinase Cdelta in the Golgi complex. J Biol Chem. 2004;279:12668-12676.

56. Cortez D, Stoica G, Pierce JH, Pendergast AM. The BCR-ABL tyrosine kinase inhibits apoptosis by activating a Ras-dependent signaling pathway. Oncogene. 1996;13:2589-2594.

57. Druker BJ, Tamura S, Buchdunger E, et al. Effects of a selective inhibitor of the Abl tyrosine kinase on the growth of Bcr-Abl positive cells. Nat Med. 1996;2:561-566.

58. Bueno-da-Silva AE, Brumatti G, Russo FO, Green DR, Amarante-Mendes GP. Bcr-Abl-mediated resistance to apoptosis is independent of constant tyrosine-kinase activity. Cell Death Differ. 2003;10:592-598.